DCB TEST SAMPLE DESIGN FOR MICRO-MECHANICAL TESTING

S. Zike, L. P. Mikkelsen, B. F. Sørensen

Composites and Materials Mechanics Section, Department of Wind Energy, Technical University of Denmark, Risø Campus, Roskilde, Denmark

* Corresponding author (zike@dtu.dk)

Keywords: *DCB testing, micro-mechanical testing, polymer fracture, polymer modeling*

1. Introduction

Application of composite materials based on polymer matrix and inorganic fibers is continuously increasing in high performance structures such as airplanes, wind turbines etc. Further development and improvement of structural performance is highly dependent on understanding of damage initiation and damage evolution in composite materials. An overview of composite material failure affected by micro-scale processes as fracture both in matrix and fiber, fiber-matrix de-bonding, pull-out of fibers etc. is discussed by Kim and Mai [1].

Damage evolution at micro-scale can be evaluated combining micro-mechanical testing *in situ* with visual observation methods as optical and electron microscope. Some review papers regarding micro-mechanical testing are given by Hemker and Sharpe [2], and Srikar and Spearing [3]. An example of micro-mechanical testing with *in situ* visual observation methods for polymer matrix based composites is given by Schoβig et al. [4]. These authors conduct micro-tension tests for polymer/glass fiber composites in an environmental scanning electron microscope (ESEM) in order to correlate visually observed damage with the signals of acoustic emission.

A comprehensive study on fracture testing in micro-scale utilizing double cantilever beam (DCB) specimens subjected to pure bending inside ESEM is done by Sørensen et al. [5–8]. They present stable crack growth in ceramics and composite materials enabling *in-situ* observations of crack growth mechanisms and material toughness variations.

The aim of this study is to determine the optimal DCB test specimen configuration for polymer materials for micro-mechanical testing inside optical microscope and ESEM. The optimal specimen design is found by conducting numerical parameter study with finite element method (FEM) code. For the fracture analysis the J integral is used [9], since this approach is valid to analyze an onset of crack growth of non-linear materials [10]. A parameter variation of DCB test specimens is done accordingly to requirements and restrictions listed in section 2.

2. DCB test requirements and restrictions

The design of DCB test specimen requires finding the balance between DCB fixture restrictions, material properties and conditions of reliable fracture parameter determination. The specimen design is done as a pre-study for experimental testing of samples made of thermoset and thermoplastic material, respectively, with properties defined in Table 1.

Experimental setup requires to operate with DCB test fixture described by Sørensen et al. [7] Fixture restricts specimen dimensions to 70 x 10 x 5 mm^3 as it is shown in Fig. 1. The total deflection of specimen is limited to 15 mm and the minimum crack length is > 12+1 mm.

Regarding fracture parameter determination following requirement are set:

1. Pure bending

   Pure bending is considered to be a prerequisite to ensure stable crack growth under constant test rate, what allows determination of actual material toughness properties. In the case of unstable crack growth, fracture parameters will be related to crack initiation and more sensitive to initial conditions as pre-crack sharpness. This can lead to determination of fracture parameters,

which are significantly higher than actual material fracture resistance [7], [11].

2. Sufficiently high J integral values

   The specimen design should be such that the J integral values are high enough to induce crack growth. Polymer materials tend to exhibit tough behavior, thus relatively high J integral values can be needed. In addition, the effect of yielding around the crack tip on the J integral determination is evaluated.

3. Stress free rear end

   A stress free rear end in the test sample is required to consider the J integral independent on the crack length. In addition, stresses at the rear end are used to evaluate the bending.

4. No buckling

   During the DCB tests, the crack tip is experiencing tension and a field with compression exists further ahead in the uncracked part of the test sample. This study is focused on soft and relatively thin materials with thickness in range of 0.75 – 1 mm. Based on these assumptions, initially, it is expected that specimens could be prone to buckling in compression dominated area.

3. Methods

3.1 Computational model

A 3D model is created to mimic the experimental set-up for Mode I DCB fracture test described by Sørensen et al. [7] using the commercial FEM code *ABAQUS*. Fig. 2 shows the corresponding numerical model of the DCB test specimen. The specimen is divided into two parts: sample and sample holder beams, also noted as skins. Parts are defined as linear-elastic and elastic-plastic.

A crack is created by partitioning sample in the middle and nodes of partitioned area are separated by assigning seems. The J integral value is determined at the crack tip by averaging 3^{rd}-5^{th} contour values.

Bending moment in the model is created applying two concentrated forces (F) pointed in opposite directions along x direction and equally applied to each skin. The force is equally distributed along the width of the skin introducing constraints (*equation constraints*). In addition, the linear perturbation testing procedure is set to predict buckling load during the DCB test.

Boundary conditions are set to restrict skins movement in z direction, the test sample surface at the rear end in y direction and the middle point of the same surface in x direction.

A reference point with kinematic constraints is set at the upper corner of the skin beam in order to measure deflection in x axis direction. The total deflection is the sum of deflections experienced by both skin beams.

A structured mesh is used for skins and sweep mesh is used for sample with an eight node linear brick elements including reduced integration and hourglass control.

3.2 Parameter study

A parameter study is conducted to design the DCB test specimen for polymer material testing. The study is focused on two specific samples one made of thermoset and another from thermoplastic material with properties listed in Table 1. Therefore to satisfy in section 2 listed requirements and restrictions for the DCB test specimen, following parameters are varied:

1) Elastic modulus of skin (E_{skin});
2) Thickness (t_{skin}) and width (h_{skin}) of skin;
3) Width of sample (h_{sample});
4) Crack length (L_{crack}).

4. Results

Results of the DCB test specimen design for polymer materials are summarized in the following steps:

1) Design of skins;
2) Determination of appropriate crack length;
3) Estimation of compression stresses at the rear end;
4) Evaluation of yielding around the crack tip;
5) Buckling analysis.

4.1 Design of skins

The sample holders are included in the DCB test specimen configuration to control the stress field around the crack tip, to limit the beam deflection and

rotation, and also to ensure the test sample is subjected to pure bending. Results regarding skin design are mostly focused on determining appropriate skin material stiffness, because variations of geometrical dimensions are very much limited by the available DCB test fixture [7].

4.1.1 J integral determination

First the effect of skin stiffness on the J integral value is evaluated. In Fig. 3 the J integral values are shown as a function of the elastic modulus of skin material (E_{skin}) for both samples made of thermoset and thermoplastic material. In addition, FEM results are compared with analytical J integral calculations for the DCB test specimens provided by Goutianos et al. [8], [11].

In Fig. 3 obtained results show that the J integral value is decreasing with stiffer skin material. Moreover, in certain range almost linear correlation between the J integral and the elastic modulus of skin material exist. This is true for specimens with relatively much stiffer skins than sample, whereas implementing softer skins deviation from linearity is observed. Deviation is more pronounced for the thermoset sample, which is stiffer and has initial elastic modulus 3 GPa. Similarly, deviations increase for wider and thicker samples. Numerical results are found to be in a good agreement with analytical model provided by Goutianos et al. [11].

In order to ensure that crack growth occurs, the J integral value (J_c) for thermoset sample should be around 0.1-1 kJ/m^2 and for thermoplastic sample around 20 kJ/m^2 [12]. In Fig. 3 results indicate that for the thermoplastic sample the elastic modulus of skin material should be below 4 GPa, to obtain desired J integral values if skin dimensions are 70 x 4 x 3 mm^3 and applied load is 75 N. In the case of the thermoset sample, selection of skin material is less critical due to stiffer sample material and much lower J integral values, thus a skin with stiffness up to 70 GPa can be used.

4.1.2 Limitations of deflection

Second the effect of skin stiffness on the total deflection is evaluated. Usage of soft skins is limited by the maximum allowable deflection (15 mm) by the DCB test fixture. Fig. 4 presents numerical results of the DCB test specimen deflection variations with product of elastic modulus and moment of area of skins (I_{skin}) when maximum load 75 N is applied. Results also include the effect of crack length for 6 mm wide (h_{sample}) thermoplastic sample using 3 mm thick (t_{skin}) and 4 mm wide (h_{skin}) skins - I_{skin} = 9 mm^4.

The results in Fig. 4 demonstrate that the total deflection is reduced linearly with stiffer skins, i. e. with larger product of I_{skin} and E_{skin}, and shorter crack. To satisfy the restrictions of the DCB test fixture the product of E_{skin} and I_{skin} should be at least 25 GPa·mm^4 and 100 GPa·mm^4 for 19 and 34 mm long crack (L_{crack}), respectively. Accordingly to results in Fig. 4, the elastic modulus of skin for the thermoplastic sample should be at least 2.8 GPa and 10 GPa for L_{crack} = 19 mm and L_{crack} = 34 mm, respectively. The thermoset sample is much stiffer and in both cases does not exceed the deflection limitations.

4.2 Crack length

In subsection 4.1., it was shown that the requirement of sufficiently high J integral value and the restrictions of deflection can be fulfilled choosing appropriate crack length. In this subsection, the J integral value variations with the crack length are discussed in order to determine the range of the crack length, which allows stable crack growth and is independent on the sample length and test fixture configuration.

In Fig. 5 the normalized J integral is shown as a function of the crack length for the specimens with different ratio of sample and skin stiffness. Initially a 1 GPa stiff, 6 mm wide and 70 mm long sample is chosen. Normalized J integral is calculated dividing numerically obtained J integral values with analytically determined using model provided by Goutianos et al. [8], [11]. The crack length is varied from 14 to 60 mm. The minimum allowable crack by the DCB test fixture is 12+1 mm.

From Fig. 5 it can be seen that the normalized J integral is constant and equal to 1 in the certain range of the crack length. This distance is enclosed by the minimum and the maximum crack length, where the normalized J integral starts to deviate from one. The minimum crack length for the specimen with the skin stiffness 1 GPa, i.e. E_{sample}/E_{skin} = 1, is found at L_{crack}/L_{sample} = 0.39, i.e. the crack length is approximately 27 mm. The total

deviation of the normalized J integral at L_{crack} = 14 mm is around 5 %. The minimum crack length is not found for the specimens with relatively stiff skins as 20 GPa and 200 GPa in the prescribed crack length region.

Significantly larger deviations from 1 are observed increasing the crack length above the maximum value. The obtained maximum crack length is in the range of 35 mm to 57 mm depending on the skin material stiffness. For the specimens with 200 GPa stiff skins, the maximum crack length is obtained at shorter distance, i.e. 35 mm, whereas the length of maximum crack increases implementing softer skins. The largest maximum crack length is obtained for the specimen with 1 GPa stiff skins.

4.3 Compression stresses at the rear end

Compression stresses develop in a region ahead of the crack tip. It is considered that less the skins will deflect the larger area of crack free region in the test sample will be subjected to compression. Therefore, initially, it is expected that for very stiff skins as 200 GPa, the specimens will not be subjected to pure bending as the test samples are relatively soft and will not provide sufficient resistance needed to bend the skin beams.

In Fig. 6 the length of the compression zone is shown as a function of the elastic modulus of the skin material for an applied load of 15 N. The results are obtained for 4 mm wide samples using skins with dimensions 70 x 3 x 3 mm^3. Numerical results present that thermoplastic samples will be more compressed comparing to thermoset sample using the skins with the same stiffness. For example, implementing 10 GPa stiff skins the compression zone size for thermoplastic sample is 40 % and for thermoset sample 25 % from total crack free region. Further increasing the skin material stiffness to 200 GPa, compression zone enlarges to 70 % and 47 % from total crack free region for thermoplastic and thermoset sample, respectively. In addition, it is seen that compression region distances from the crack tip with stiffer skin material.

4.4 Evaluation of yielding around the crack tip

The effect of yielding around the crack tip on the J integral determination is assessed for specimens with E_{skin} = 3 GPa and skin beam dimensions 70 x 3 x 3 mm^3. Skins in both samples ensure sufficiently high J integral value and fulfill the restrictions of deflection implementing 19 mm long crack. Evaluation is done comparing three material configurations as listed below:

1) *Elastic-elastic*, where the linear-elastic material properties are used both for sample and skin. The "size of plastic zone" is evaluated solely on the elastic strain contour.
2) *Plastic-elastic*, where the plastic yielding of the sample material is included and the skins remain elastic.
3) *Plastic-plastic*, where the plastic deformation of the sample and the skin material is included. Thus the effect of the test sample and the skin material yielding on the J integral assessment is evaluated.

In Fig. 7 the J integral variations with the deflection for different material formulations are presented for the thermoset sample. The results show that the yielding of the sample and the skin material does not affect the J integral determination up to J = 1 kJ/m^2 with the total deflection 2 mm. The deviations tend to increase with increasing the deflection. For instance, the difference between the J integral value obtained by the elastic-elastic and the plastic-plastic material formulation is approximately 0.5 kJ/m^2 for the total deflection 3 mm. The size of plastic zone is not found to be affected by the plastic deformation of the skin and the test sample material if J = 1 kJ/m^2. The length of the plasticity zone around the crack tip is 1.5 mm both in the direction of the crack tip and transverse to it.

A similar approach is used to evaluate the effect of yielding on the J integral determination for the thermoplastic sample. In Fig. 8 it is shown that for the thermoplastic material the J integral variations with deflection using the elastic-elastic and the plastic-plastic material formulation coincidence up to J = 5-7 k J/m^2. Large deviations are observed at critical J integral value - J = 20 kJ/m^2 [12]. The numerically determined plasticity zone size is 9.5 mm if J = 20 kJ/m^2 for 4 mm wide sample. A widening of the sample till 10 mm slightly increase the J integral values, nevertheless the plasticity zone is still spread along the whole width of test sample.

4.5 Buckling analysis

Buckling analysis is conducted for both thermoplastic and thermoset sample in order to predict the sample buckling during DCB test. In addition, numerical results are compared with Euler beam buckling predictions.

4.5.1 Euler buckling

Euler buckling stress is determined for the crack free region assuming both ends are pinned. Skin properties are not included in calculations. The Euler buckling stress is found to be 3.2 MPa if E_{sample} = 250 MPa, t_{sample} = 0.75 mm and width is 6 mm. The buckling stress value is increased up to 7.2 MPa if the width is reduced to 4 mm. Significantly higher buckling stress values as 38 MPa are obtained for the thermoset sample with E_{sample} = 3 GPa, t_{sample} = 1 mm and h_{sample} = 6 mm.

4.5.2 Numerically determined buckling

Numerically obtained buckling results are shown in Fig. 9 for 6 mm wide thermoplastic sample. Both the buckling load and the maximum stress at the first stable buckling mode are shown as function of the skin stiffness in the range of 1-200 GPa. Buckling threshold equals to the maximum load allowable by DCB test fixture – 75 N.

In Fig. 9 results indicate that the buckling of sandwich type DCB test specimen is significantly affected by the skin stiffness. Usage of stiffer skins leads to larger buckling loads and lower compression stresses in the crack free region. Results show that to avoid the buckling in thermoplastic sample the elastic modulus of the skins should be above 3 GPa. In Fig. 9 the Euler buckling stress is included for this sample, which is approximately 4 times lower than the numerically determined if the test sample with 2 GPa stiff skins is considered.

In the range of skin stiffness 1-200 GPa no buckling is observed neither for the thermoplastic sample with h_{sample} = 4 mm nor the thermoset sample with h_{sample} = 4 mm and h_{sample} = 6 mm.

Additionally, in Fig. 10 the first stable buckling mode is shown for 6 mm wide thermoplastic sample with 3 GPa stiff skins. It is observed that with increasing stiffness of the skin material, the buckled area widens and tends to move away from the crack tip, therefore if E_{sample} = 0.25 GPa and E_{skin} = 200 GPa buckling will occur at the end of the crack free region of test sample.

5. Discussion

5.1 Skin selection

Results in Fig. 3 and Fig. 4 show that the stiffness of skins highly affects the stress concentration at the crack tip and also the deflection of specimen beams. Softer skins promote higher stress localization close to the crack tip leading to higher J integral values. With increasing skin stiffness, the compression region increases, thus stresses tend to be more delocalized, and the values of the maximum compression stress and the J integral value are reduced, see Fig. 5.

In Fig. 3 for stiff skins linear relation between J integral and elastic modulus of the skins can be observed. Deviations from the linear correlation between the J integral and the skin stiffness are observed reducing the elastic modulus of skin. Deviations from linearity become more pronounced for stiffer, wider and thicker sample, thus sample properties more significantly start to affect total bending of outer beams.

Besides larger J integral values, the implementation of soft skins leads to larger deflections, which then can be reduced by shortening the crack as shown in Fig. 4. Two lengths of crack are compared showing that for thermoplastic sample the 19 mm long crack is preferable as deflection restrictions are satisfied. The thermoset sample is much stiffer and in both cases does not exceed the deflection limitations.

To satisfy both requirements of sufficiently high stresses at the crack tip and deflection restrictions, it is proposed that for thermoplastic sample with skin dimensions 70 x 4 x 3 mm^3 E_{skin} should be in the range of 2.8 - 4 GPa. Thus skins made of polymer materials, e.g. made of epoxy, are suggested.

5.2 Crack length limitations

In Fig. 5 the effect of crack length on the J integral determination is presented. The range of optimal crack length, when J integral value is not affected by the sample dimensions and the crack tip is loaded under pure bending, is confined by minimum and maximum crack length. Inside this region, the

normalized J integral value is constant and equal to one. The deviations below the minimum crack are considered to be small comparing to the values above the maximum crack length. Furthermore, it is found that the maximum crack is shorter for specimens with stiffer skin material, and also the range of the constant J integral value is reduced. These observations are explained with more localized stresses, and thus smaller compression area in the uncracked part of sample, using soft skins, see Fig. 6.

5.2 Yielding at the crack tip

The plastic deformation of the test sample and the skin material is included to evaluate the effect of yielding on the J integral determination. No effect of plastic deformation on the J integral value is observed for the thermoset sample up to 1 kJ/m^2, see Fig. 7. The same J integral values are obtained using elastic and elastic-plastic material formulation both for the skin and the test sample. Thus the effect of yielding around the crack tip for thermoset sample is considered to be small.

Considerably different results are attained for the thermoplastic sample shown in Fig. 8. Defining the test sample and the skin as a linear-elastic material the critical J integral 20 kJ/m^2 is achieved at total deflection 14 mm. Including the plastic deformation of the sample and the skin J integral values are reduced to half for the same deflection. The plasticity zone is found to be 9.5 mm long if J = 20 kJ/m^2 and sample width 4 mm. Moreover, widening the sample till 10 mm is not sufficient to reduce the effect of plastic deformation. In both cases, the observed plasticity zone exceeds the test sample width.

5.3 Buckling

Numerical results presented in Fig. 10 show the local type of buckling what is largely affected by the utilized skins. Stiffer skins tend to delocalize stresses and therefore increase required load to induce buckling. Applying skins with elastic modulus E_{skin} = 3 GPa, what satisfies requirement of high stress concentration at the crack tip and the restrictions of deflection, numerically no buckling is expected for both thermoplastic and thermoset samples either 4 mm or 6 mm wide, see Fig. 9. In all cases, to induce buckling externally applied load has to be larger than 75 N, what is the limit of fixture.

In addition, numerical buckling results for specimens with E_{skin} = 3 GPa and E_{sample} = 250 MPa are compared to Euler beam buckling stresses. In this case, Euler buckling stress values are attained to be much smaller than the numerically obtained maximum compression stress for 6 mm and 4 mm wide thermoplastic samples, respectively. Therefore, in this study, Euler beam buckling formulation is considered to be too conservative for buckling evaluation in DCB test samples.

Conclusions

Thermoplastic sample

1) The elastic modulus of skin should be below 4 GPa to obtain the required J integral values. Due to relatively soft skins large deflections are expected, therefore 19 mm long crack is recommended.
2) J integral values are strongly affected by the plastic deformation of the test sample and the skin material. The yielding is not small scale. The determined plastic zone is 9.5 mm.
3) Thermoplastic samples are not prone to buckling in the range of dimension limitations if epoxy based skins are chosen.
4) Euler beam buckling formulation is too conservative to predict buckling stresses for this study.

Thermoset sample

1) Skin selection is less critical than for the thermoplastic sample because the critical J integral values are lower and are achieved at rather small deflections.
2) Deflection does not exceed DCB test fixture limitations both implementing 19 mm and 34 mm long crack.
3) Yielding around the crack tip is found to be small. Fracture parameter determination can be based on elastic material formulation as the effect of plastic deformation is not found. The determined plastic zone is 1.5 mm.

4) Buckling is not expected using skins with elastic modulus 3 GPa.

References

[1] J. Kim and Y. Mai, "High strength, high fracture toughness fibre composites with interface control—a review," *Composites Science and Technology*, 1991.

[2] K. J. Hemker and W. N. Sharpe, "Microscale Characterization of Mechanical Properties," *Annual Review of Materials Research*, vol. 37, no. 1, pp. 93–126, Aug. 2007.

[3] V. T. Srikar and S. M. Spearing, "A Critical Review of Microscale Mechanical Testing Methods Used in the Design of Microelectromechanical Systems," *Experimental Mechanics*, vol. 43, no. 3, pp. 238–247, Sep. 2003.

[4] M. Schoßig, A. Zankel, C. Bierögel, P. Pölt, and W. Grellmann, "ESEM investigations for assessment of damage kinetics of short glass fibre reinforced thermoplastics – Results of in situ tensile tests coupled with acoustic emission analysis," vol. 71, pp. 257–265, 2011.

[5] A. N. Kumar and B. F. Sørensen, "Fracture Resistance and Stable Crack-Growth Behavior of 8-mol%-Yttria-Stabilized Zirconia," *Journal of the American Ceramic Society*, vol. 83, no. 5, pp. 1199–1206, 2000.

[6] B. F. Sorensen and A. Horsewell, "Crack Growth along Interfaces in Porous Ceramic Layers," *Journal of the American Ceramic Society*, vol. 84, no. 9, pp. 2051–59, 2001.

[7] B. F. Sørensen, A. Horsewell, O. Jørgensen, A. N. Kumar, and P. Engbæk, "Fracture resistance measurement method for in situ observation of crack mechanisms," *Journal of the American Ceramic Society*, vol. 81, no. 3, pp. 661–669, 1998.

[8] S. Goutianos, R. Arevalo, B. F. Sørensen, and T. Peijs, "Effect of Processing Conditions on Fracture Resistance and Cohesive Laws of Binderfree All-Cellulose Composites," *International Journal of Solids and Structures*, 2013.

[9] J. Rice, "A path independent integral and the approximate analysis of strain concentration by notches and cracks," vol. 35, pp. 379–386, 1967.

[10] N. Fleck and J. Hutchinson, "A phenomenological theory for strain gradient effects in plasticity," *Journal of the Mechanics and Physics of Solids*, vol. 41, no. 12, pp. 1825–1857, 1993.

[11] S. Goutianos, H. L. Frandsen, and B. F. Sørensen, "Fracture properties of nickel-based anodes for solid oxide fuel cells," *Journal of the European Ceramic Society*, vol. 30, no. 15, pp. 3173–3179, Nov. 2010.

[12] A. J. Kinloch and R. J. Young, *Fracture behaviour of polymers*. Applied Science Publishers, 1983.

Acknowledgments

This research was supported by the Danish Centre for Composite Structure and Materials for Wind Turbines (DCCSM), grant no. 09-067212, from the Danish Strategic Research Council (DSF).

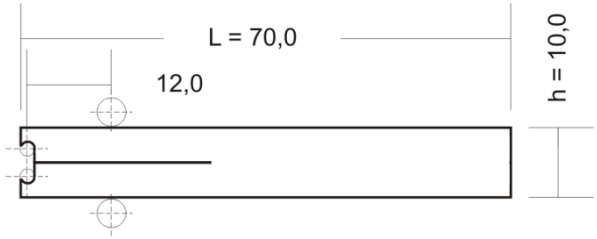

Fig. 1. The DCB test specimen dimensions

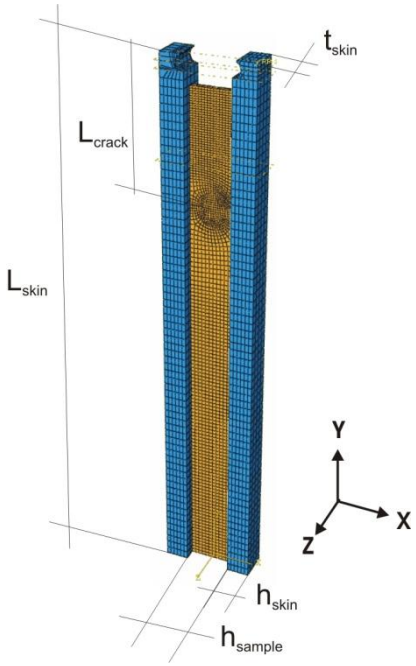

Fig. 2. DCB model used in numerical calculations

Table 1. Material properties of samples

	Thermoplastic	Thermoset
E_{sample}, GPa	0.25	3
σ_{yield}, MPa	10	26.5
$\varepsilon_{ultimate}$, %	78.5	7.8
t_{sample}, mm	0.75	1
G_{IC}, kJ/m^2 [12]	20	0.1-1

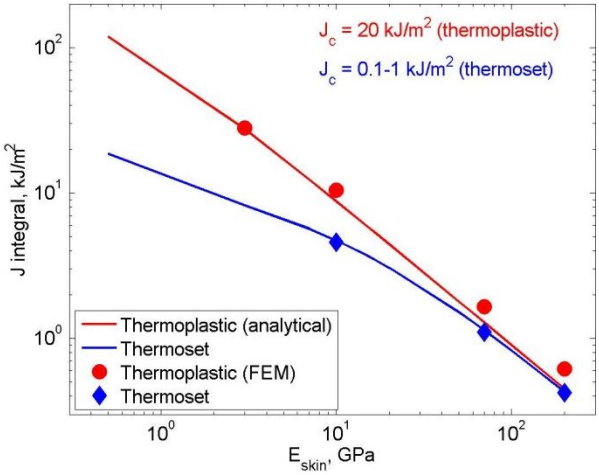

Fig. 3. Comparison between FEM and analytically [11] determined J integral variations with skin stiffness for external load 75 N

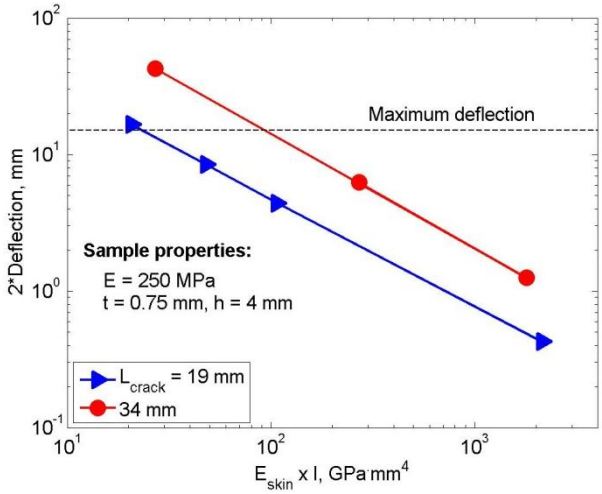

Fig. 4. Numerically obtained deflection values for the thermoplastic sample varying the crack length

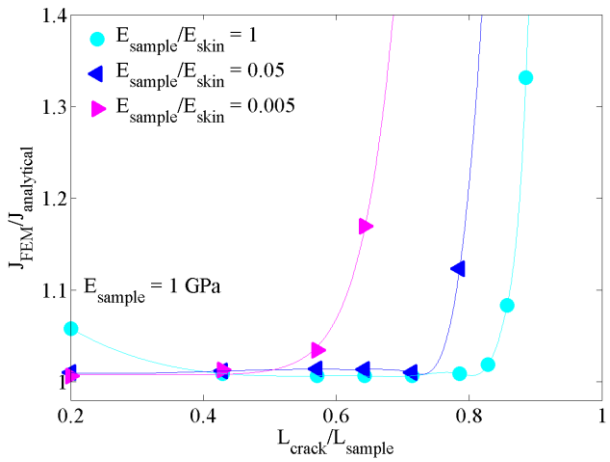

Fig. 5. Normalized J integral values versus crack length for the specimens with different skin stiffness

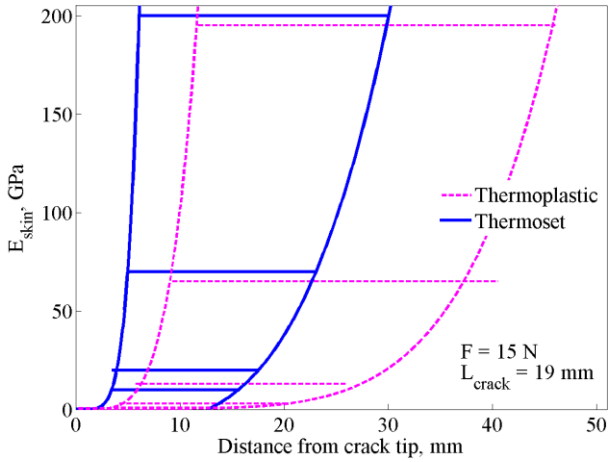

Fig. 6. The length of compressed region in the rear end of sample versus skin stiffness

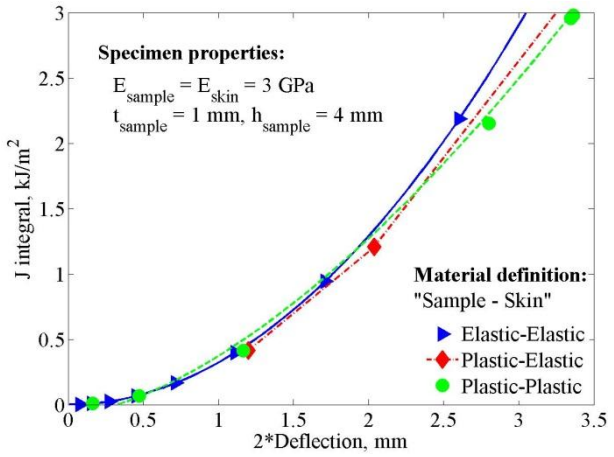

Fig. 7. J integral variations with material formulation for thermoset sample

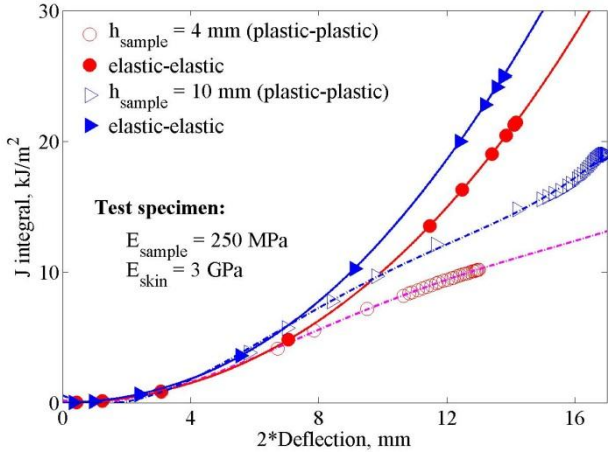

Fig. 8. J integral variations with material formulation for thermoplastic sample

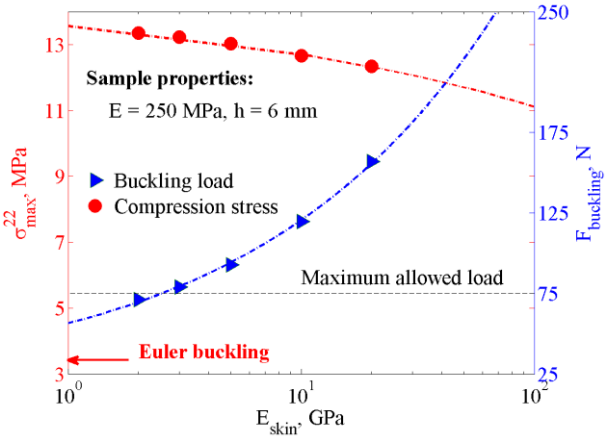

Fig. 9. Buckling results determined by FEM

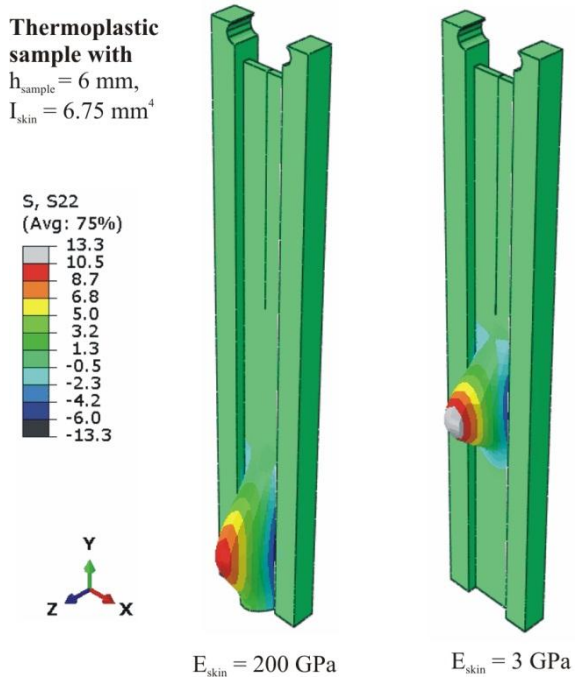

Fig. 10. Examples of stable buckling mode used for buckling result extraction